bioRxiv preprint doi: https://doi.org/10.1101/099143; this version posted January 8, 2017. The copyright holder for this preprint (which was not certified by peer review) is the author/funder, who has granted bioRxiv a license to display the preprint in perpetuity. It is made available under aCC-BY-NC-ND 4.0 International license.

Whole genome sequencing and assembly of a *Caenorhabditis elegans* genome with complex genomic rearrangements using the MinION sequencing device

Authors: Tyson JR[1*], O'Neil NJ[2*], Jain M[3*], Olsen HE[3], Hieter P[4], Snutch TP[1]

1. Michael Smith Laboratories and Djavad Mowafaghian Centre for Brain Health, University of British Columbia, Vancouver, Canada.
2. Michael Smith Laboratories, University of British Columbia, Vancouver, BC, Canada V6T 1Z4
3. UC Santa Cruz Genomics Institute and Department of Biomolecular Engineering, University of California, Santa Cruz, California, USA.
4. Michael Smith Laboratories, University of British Columbia, Vancouver, BC, Canada V6T 1Z4; Department of Medical Genetics, University of British Columbia, Vancouver, BC, Canada V6T 1Z3

ABSTRACT

Advances in 3rd generation sequencing have opened new possibilities for 'benchtop' whole genome sequencing. The MinION is a portable device that uses nanopore technology and can sequence long DNA molecules. MinION long reads are well suited for sequencing and *de novo* assembly of complex genomes with large repetitive elements. Long reads also facilitate the identification of complex genomic rearrangements such as those observed in tumor genomes. To assess the feasibility of the *de novo* assembly of large complex genomes using both MinION and Illumina platforms, we sequenced the genome of a *Caenorhabditis elegans* strain that contains a complex acetaldehyde-induced rearrangement and a biolistic bombardment-mediated insertion of a GFP containing plasmid. Using ~5.8 gigabases of MinION sequence data, we were able to assemble a *C. elegans* genome containing 145 contigs (N50 contig length = 1.22 Mb) that covered >99% of the 100,286,401 bp reference genome. In contrast, using ~8.04 gigabases of Illumina sequence data, we were able to assemble a *C. elegans* genome in 38,645 contigs (N50 contig length = ~26 kb) containing 117 Mb. From the MinION genome assembly we identified the complex structures of both the acetaldehyde-induced mutation and the biolistic-mediated insertion. To date, this is the largest genome to be assembled exclusively from MinION data and

bioRxiv preprint doi: https://doi.org/10.1101/099143; this version posted January 8, 2017. The copyright holder for this preprint (which was not certified by peer review) is the author/funder, who has granted bioRxiv a license to display the preprint in perpetuity. It is made available under aCC-BY-NC-ND 4.0 International license.

is the first demonstration that the long reads of MinION sequencing can be used for whole genome assembly of large (100 Mb) genomes and the elucidation of complex genomic rearrangements.

Introduction

Advances in Next Generation Sequencing (NGS) have ushered in a new era of whole genome analysis. The short sequencing reads generated by sequencing-by-synthesis NGS are well suited for resequencing complex genomes for which a reference sequence has been established. However, short reads are poorly suited for *de novo* assembly of complex genomes in part due to repeat regions that generate highly discontinuous assemblies and require unique flanking sequences to position repeat elements. In many instances if a sequencing read does not completely span a repeat, either due to repeat size or physical properties of the repetitive DNA, it can not be unambiguously assembled into a contig. This can pose a problem for the *de novo* assembly of metazoan genomes where repetitive elements are common. For example, approximately 12% of the 100 Mb *C. elegans* genome is derived from transposable elements (Bessereau JL. 2006). As such, NGS is not optimal for sequencing and assembly of large novel genomes or genomes with numerous complex rearrangements such as those observed in tumour cells.

Third Generation Sequencing (TGS) technologies have increased read lengths 100 to 1000-fold compared to NGS platforms and therefore can span much larger repeat regions than NGS. The first major TGS platform was the Pacific Biosciences Single Molecule Real Time (SMRT) PacBio sequencing system. PacBio sequencing averages 10 kb read lengths and with consensus sequencing the error rate approaches that of NGS. In 2014, Oxford Nanopore Technologies (ONT) introduced the MinION nanopore sequencer. The MinION directly connects to a laptop or desktop PC via a USB3 port, is ~90 grams, and costs are for reagents only. The MinION works on the principle of nanopore strand sequencing (Deamer et al. 2016). Briefly, a DNA strand is enzymatically unzipped and ratcheted through a membrane-inserted protein nanopore as a voltage potential is applied. As the DNA single strand translocates, the resulting changes in ionic current are measured and sequence calls produced corresponding to the identity of the

bioRxiv preprint doi: https://doi.org/10.1101/099143; this version posted January 8, 2017. The copyright holder for this preprint (which was not certified by peer review) is the author/funder, who has granted bioRxiv a license to display the preprint in perpetuity. It is made available under aCC-BY-NC-ND 4.0 International license.

nucleotides via computationally inferred model fitting. When only one strand (template) from a duplex DNA molecule is read by the nanopore, the resulting sequence call is termed a 1D read (Jain *et al* 2016). With certain library preparations an optional hairpin strand bridge provides the opportunity to sequence both strands of a dsDNA (template and complement) generating a 2D read, which results in a higher accuracy sequence call. MinION sequence read lengths range from several hundred bases to hundreds of thousands of bases, and are essentially limited by the DNA preparation type and delivery to the pore. Early versions of the MinION sequencing chemistry and base calling produced sequences with relatively high error rates (22-35%) when compared to both NGS (<2%) and PacBio TGS (10-15%). The high error rate combined with relatively low sequencing yields per flow cell (<1 Gb/flow cell) led some researchers to underestimate the potential for this technology. Recent advances in the MinION chemistry and base calling have greatly improved accuracy (5-10% error rate) and yield (2-5 Gb/flowcell) (J. Tyson unpublished results). To date, most studies have used the MinION to sequence small genomes or to partially survey larger genomes to assess chromosomal structure and copy number variations (Loman et al. 2015, Goodwin et al. 2015, Norris et al. 2016, Wei & Williams 2016,). The long read lengths of this technology, combined with recent improvements in performance make the MinION a viable option for whole genome sequencing of complex metazoan genomes.

The *Caenorhabditis elegans* genome was the first metazoan genome to be completely sequenced (*C. elegans* Sequencing Consortium 1998) and is an excellent model genome for assessing new whole genome sequencing technologies. The *C. elegans* genome is complex with many different types of local and dispersed repeat sequences in both intronic and intergenic regions and only 27% of the genome residing in exons. Local repeats range from short repetitive sequences such as homopolymeric G tracts (Zhao et al. 2007) to large tandem repeats spanning tens of kilobases. The most common dispersed repeats are derived from transposable elements and constitute approximately 12% of the genome (Bessereau 2006). *C. elegans* transposons range in size from 1-3 kb and can confound genomic assemblies as transposon sequences are larger than NGS and Sanger sequencing reads resulting in ambiguous mapping positions. The assembly of the *C. elegans* reference genome was made possible by the construction of a high quality physical map of cosmids and yeast artificial chromosomes (Coulson et al. 1988; Coulson et al. 1995; Coulson

bioRxiv preprint doi: https://doi.org/10.1101/099143; this version posted January 8, 2017. The copyright holder for this preprint (which was not certified by peer review) is the author/funder, who has granted bioRxiv a license to display the preprint in perpetuity. It is made available under aCC-BY-NC-ND 4.0 International license.

et al. 1991), which were individually shotgun sequenced and manually finished to bridge gaps and ambiguous regions to generate a complete high quality reference genome (C. elegans Sequencing Consortium 1998). The high-quality reference genome has facilitated studies using NGS re-sequencing to aid identifying new mutants and analysing mutational profiles (Thompson et al. 2013; Meier et al. 2014). Nevertheless, the potential for assembly discrepancies using NGS in sequence determination remain and NGS is not optimal for *de novo* genome assembly or understanding large structural alterations such as those associated with cancer and complex genetic disorders.

Here, we report the sequencing and *de novo* assembly of a 100 Mb *C. elegans* genome exclusively from MinION reads. For comparison, we used both MinION and Illumina platforms to sequence the genome of a *C. elegans* strain containing both a complex genome rearrangement generated by acetaldehyde mutagenesis and a ballistic-mediated insertional event of a GFP-containing plasmid (*him-9(e1487);ruIs32*). The *de novo* assembly of MinION data generated a remarkably complete genome in 145 contigs that cover >99% of the reference genome with an N50 contig length of 1.22 Mb. Furthermore, the sequence assembly elucidated the complex structure of the rearrangement and insertion events that were not readily apparent in the Illumina data. The strategy of comparison to Illumina data was however useful to improve the sequence accuracy of the MinION assembly. Together, this hybrid sequencing approach generated a physical map with high sequence accuracy and further represents the largest genome assembled exclusively from MinION data.

Materials and Methods

Nematode culture and DNA extraction

Nematodes were cultured as previously described (Brenner 1974). The *him-9(e1487)* II; *unc-119(ed3) ruIs32[pie-1p::GFP::H2B + unc-119(+)]* III strain was constructed by mating CB1487 *him-9(e1487)* males to AZ212 *unc-119*(*ed3*) *ruIs32* III hermaphrodites. F1 heterozygotes were selfed and *him-9; ruIs32* homozygotes isolated. Worms were grown to starvation for sequencing on NGM plates and harvested by washing with M9 buffer and pelleted in 15-ml centrifuge tubes. Buffer was removed by two washes with sterile distilled water, centrifugation and aspiration.

bioRxiv preprint doi: https://doi.org/10.1101/099143; this version posted January 8, 2017. The copyright holder for this preprint (which was not certified by peer review) is the author/funder, who has granted bioRxiv a license to display the preprint in perpetuity. It is made available under aCC-BY-NC-ND 4.0 International license.

The worm pellet was resuspended in 300 µl of lysis buffer (200 mM NaCl, 100 mM Tris-HCl pH 8.5, 50 mM EDTA pH 8.0, 0.5% SDS, 0.1 mg/ml proteinase K) and frozen at -80 ^{o}C. Frozen pellets were incubated at 60 ^{o}C for 1-3 hours followed by 95°C for 20 minutes. RNase A (0.1 mg/ml) was added and lysed worms were incubated at 37°C for 1 hour. DNA was prepared by standard phenol/chloroform extraction and DNA was resuspended in 10 mM Tris pH 8.0.

Library Preparation and MinION Sequencing

The Chip84-Chip90 MinION flowcells were run using libraries prepared with the SQK-NSK007 Nanopore Sequencing Kit R9 version. Chip94 & Chip95 libraries were prepared using the SQK-RAD001 Rapid Sequencing Kit I R9 version. The standard protocols from Oxford Nanopore Technologies were used with the following modifications. For SQK-NSK007 libraries, purification of DNA after the FFPE treatment step was done using 0.4x AMPureXP beads. Prior to adapter ligation each elution step off the AMPureXP beads was performed using 10 mM Tris pH 8.0, instead of water, at 37°C for 5 mins. The starting amounts of gDNA ranged between 0.8 µg and 2.0 µg (see Table S1 for details). Priming of individual flowcells with running buffer (2x 500 µl) and sequencing library top ups (150 µl) were performed at times detailed in Table 1. Flowcells were run for ~48 hrs using custom device tuning scripts. The tuning scripts provide event yield monitoring aimed at maintaining data throughput through initiation of a maximal pore channel assignment/usage strategy and optimal bias-voltage selection via methods outlined below.

Modified MinION running scripts

After initial start of a MinION sequencer run using the standard ONT sequencing scripts, MinION sequencing control was shifted to a custom MinKNOW MinION script to enhance pore utilisation and increase data yields. This custom script adjusted a number of run/flowcell metrics and parameters including-

1) Initiation of a bias-voltage re-selection and active pore re-population into active channels when the hourly event yields falls below a threshold. This threshold was set at 67% of the first hour of each particular sequencing segment, and generally ran for 2-5 hours per segment.

bioRxiv preprint doi: https://doi.org/10.1101/099143; this version posted January 8, 2017. The copyright holder for this preprint (which was not certified by peer review) is the author/funder, who has granted bioRxiv a license to display the preprint in perpetuity. It is made available under aCC-BY-NC-ND 4.0 International license.

2) Identifying the bias-voltages that provide the greatest number of active pores by scanning a voltage range (20-30 mV in increments of -10 mV) and using this for active pore channel re-assignment. A newly selected bias-voltage acts as the starting point for subsequent scans, and provides an active pore "tracking" ability as the required bias-voltage magnitude increases during a run with the electrochemical gradient decay of individual wells. This re-assignment also provides access to the full 2048 possible wells repeatedly throughout a run.

3) Selecting a lower magnitude bias-voltage wherein the active pore numbers are within 10% of the peak voltage. Keeping greater pore numbers active using these approaches results in wells/pores running for different periods of time and the bias-voltage requirement to drive the same current through a pore increase and diverge with use. This is because the electrochemical gradient of active wells/pores decays at a greater rate than that of inactive wells/pores. By using off peak, lower magnitude bias-voltage selection, a measure of pore population containment or "shepherding" is provided by moving lower magnitude voltage requiring pores into the rest of the population.

For further details on these device running script modifications see, https://community.nanoporetech.com/posts/r9-tuning-scripts-for-mink, and links contained within.

Base-calling MinION Sequencing Reads

All reads generated from the MinION sequencing device were base-called using the cloud-based Metrichor service provided by Oxford Nanopore. Details of specific versions can be found in Table S1 for the different runs. DNA sequences were extracted from individually called reads using simple python scripts and combined in a single fasta file format of a particular strand sequence type. Runs using the SQK-NSK007 (2D) kit generated template and a fraction of complement and 2D sequence from individual reads. SQK-RAD001 (1D) Library runs generated template (1D) reads. Filtering based on a quality metric by Metrichor divided the reads additionally into 'pass' and 'fail' categories. Some or all these sequence containing files for each run were then used for genome assembly as indicated.

bioRxiv preprint doi: https://doi.org/10.1101/099143; this version posted January 8, 2017. The copyright holder for this preprint (which was not certified by peer review) is the author/funder, who has granted bioRxiv a license to display the preprint in perpetuity. It is made available under aCC-BY-NC-ND 4.0 International license.

Genome assembly and evaluation

SPAdes Illumina assembly

For Illumina data, low quality bases were trimmed from both ends using seqtk (lh. lh3/seqtk. *GitHub* Available at: https://github.com/lh3/seqtk. (Accessed: 26th November 2016)). The threshold used for trimming was a quality score of 30. We performed an Illumina only assembly using SPAdes (Nurk et al. 2013) in its default settings with kmer sizes 21, 51, and 71. The number of threads used was 32 with a memory of 156 GB.

Canu nanopore assembly

We pooled all the nanopore data (pass and fail; 1D and 2D) and filtered out reads below a size of 1 kb to avoid overlap detection issues. The remainder of reads (~6.03 gigabases) were assembled using Canu (Koren et al. 2016) in its default settings.

Assembly correction

The Canu assemblies were corrected using Pilon (Walker et al. 2014) using recommended settings to polish for variants and homopolymers. We did not perform quality filtering on the Illumina data and all of the ~8.04 gigabases of short read sequence was used.

Nanopore data and assembly evaluation

Nanopore reads and assemblies were evaluated by alignment against the reference worm genome using marginAlign version 0.1 (with BWA-MEM (Li 2013)) (Jain et al. 2015). Alignment and error statistics were computed using marginStats version 0.1 (Jain et al. 2015). To better estimate the errors for nanopore data, we improved the alignments using marginAlign EM (Jain et al. 2015). We also performed secondary evaluations using LASTZ alignments to align draft assemblies against the reference.

We evaluated the assembly quality by using QUAST (Gurevich et al. 2013) with recommended settings and the reference worm genome. We compared changes in indels and mismatches for the Canu assemblies before and after Pilon correction. We evaluated the assemblies based on: 1) the total number of aligned bases in the assembly; 2) the number of mismatches; and 3) the total number of bases contained in indels.

bioRxiv preprint doi: https://doi.org/10.1101/099143; this version posted January 8, 2017. The copyright holder for this preprint (which was not certified by peer review) is the author/funder, who has granted bioRxiv a license to display the preprint in perpetuity. It is made available under aCC-BY-NC-ND 4.0 International license.

Results

Sequencing a *C. elegans* strain with complex rearrangements

To assess the feasibility of using MinION sequencing to both generate *de novo* whole genome assemblies of large genomes and delineate complex rearrangements, we constructed for sequencing a *C. elegans* strain, *him-9(e1487)* II; *unc-119(ed3) ruIs32[pie-1p::GFP::H2B + unc-119(+)]* III, that contained two homozygous complex rearrangements. The *him-9(e1487)* mutation was induced by acetaldehyde mutagenesis (Hodgkin et al. 1979) and is a complex duplication and insertion event that disrupts the predicted *C. elegans XPF* orthologue *xpf-1* (Youds et al. 2006). Previous analysis of *him-9(e1487)* determined that the insertion contained duplicated sequence from the *mab-3* gene (N.J. O'Neil, unpublished data). However, the complex nature of the mutation stymied attempts to determine the exact structure of the rearrangement. The *ruIs32* insertion is a low-copy number insertion that was generated by biolistic transformation of the plasmid pAZ132 [*Ppie-1::GFP::H2B::pie-1*] (derived from pJH4.52) and a plasmid containing *unc-119* [*unc-119(+)*] into an *unc-119(ed3)* mutant (Wormbase). Genomic DNA was prepared from the *him-9(e1487)* II; *ruIs32* III strain and sequenced by both a MinION sequencer using R9 chemistry and Illumina sequencing using 300 base paired-end reads.

Sequencing runs from six MinION flow cells using the R9.0 (4x) and R9.3 (2x) pore flowcell types were produced on the MinION device controlled by custom tuning scripts (see Methods). This resulted in 1.1M individual reads up to 123,159 bases in length (mean = 4,801) and containing 5.33Gb of 1D bases. An additional 1Gb of 2D sequence was generated from the paired template and complement 1D reads produced from the R9.0 flow cells using the SQK-NSK007 2D chemistry and Metrichor basecaller. Details of the individual MinION sequencing runs and the MinION sequencing chemistries used can be found in (Figure 1) and (Table 1). Significant improvements in the 1D sequence quality of individual reads was observed when comparing R9.3 to R9.0 (Figure S1). This evolution on a path to the present day R9.4 pore provided significant advances in the simpler production of higher quality 1D reads approaching the percentage read identity of the previous generation 2D reads. Nanopore read quality was measured by alignment to the *C. elegans* reference genome. The median identity for pass 1D

bioRxiv preprint doi: https://doi.org/10.1101/099143; this version posted January 8, 2017. The copyright holder for this preprint (which was not certified by peer review) is the author/funder, who has granted bioRxiv a license to display the preprint in perpetuity. It is made available under aCC-BY-NC-ND 4.0 International license.

reads from the 1D runs that used SQK-RAD001 Rapid Sequencing Kit I R9 version was ~93%. The median identities for pass 2D reads from the 2D runs that used SQK-NSK007 Nanopore Sequencing Kit R9 version (Chips 84-90) ranged between 90-95%. Illumina sequencing produced 14,041,499 paired end reads totaling ~8.04 Gb of sequence (Table 2). Alignment of the MinION sequence reads to the *C. elegans* reference genome demonstrated that most of the genome was well covered (~50X coverage) and identified an apparent ~2 Mb duplication on chromosome III (Figure 2).

de novo assembly of the *C. elegans* genome from MinION and Illumina sequence reads

1D and 2D sequence reads were filtered by size to exclude reads < 1kb and Canu (Korin et al 2016) a genome assembler designed for high-noise single-molecule sequencing was used to assemble contigs. A Canu assembly was performed using all "pass" and "fail" reads from all prepared library types to generate an assembly containing 294 contigs ranging in length from 3,695 to 4,573,586 bases with an average contig size of 351 kb. The Canu contigs were polished using Pilon and the Illumina sequence data (Table 3). 145 of the contigs containing 101,982,548 bases had significant homology to *C. elegans* (Table 4). Most of the non-*C. elegans* contigs were homologous to bacterial genomes consistent with the bacteria present on the NGM petri plates used to grow the nematodes. The mean length for *C. elegans* matching contigs was 703,328 bases compared to a mean contig length of 28,266 bases for the 149 non-*C. elegans* contigs, likely due to lower coverage. The 145 *C. elegans* contigs were aligned to the WBcel235 release of the *C. elegans* reference genome using LASTZ aligner (Harris, R.S. 2007). The alignment of contigs to the six chromosomes and the *C. elegans* mitochondrial genome covered >99% of the reference genome with >97% identical sites (Table 5; Figure 3). There were no large gaps in coverage of the reference genome. Three contigs, aligned to two different chromosomes resulting in apparent discontinuities. These hybrid contigs were most likely misassembled contigs as no other evidence suggests that these regions have been translocated.

MinION generated contigs unambiguously assigned transposon locations

To assess the quality of the assembly with respect to repetitive elements, we compared the number and position of Tc1 transposons in the *him-9; ruIs32* MinION generated contigs to the

bioRxiv preprint doi: https://doi.org/10.1101/099143; this version posted January 8, 2017. The copyright holder for this preprint (which was not certified by peer review) is the author/funder, who has granted bioRxiv a license to display the preprint in perpetuity. It is made available under aCC-BY-NC-ND 4.0 International license.

reference genome. Tc1 is a 1.6 kb transposon. NGS paired end reads are not sufficiently long to span the Tc1 transposons and cannot be unambiguously mapped resulting in a mapping quality score of 0 when aligned by the BWA aligner. Transposon number and position in the assembled contigs can be used as a measure of how effective MinION long reads are for spanning dispersed repeat regions. BLAST was used to align Tc1 reference sequences to the 145 worm contigs and the *C. elegans* reference genome. All described Tc1 elements were present in the MinION contigs and corresponded to their position in the reference genome based on the LASTZ alignments. (Table 6)

MinION reads elucidated the structure of complex repetitive chromosome rearrangements

In addition to *de novo* genome assembly, long sequencing reads can also facilitate the delineation of complex chromosomal rearrangements that contain multiple breakpoints, duplications, deletions and repeated sequences. The *C. elegans* strain sequenced here possessed two different complex genome rearrangements: *him-9(e1487)* is an acetaldehyde-induced duplication-insertion event on chromosome II and *ruIs32* is a biolistic-mediated transgenic insertion on chromosome III. Previous data from oligo array hybridization, reverse transcriptase PCR, and inverse-PCR experiments suggested that *him-9(e1487)* was an insertion of approximately 20 kb of sequence from the *mab-3* region into the *xpf-1* gene. Assembly of MinION reads revealed a significantly more complex genomic rearrangement. While the insertion breakpoints were consistent with previous data, the insertion was larger than previously anticipated. In addition to the *mab-3* duplicated region, the insertion also included an inverted repeat of part of the *mab-3* duplication and the second exon of *xpf-1,* resulting in a much larger, more complex insertion than expected (Figure 4A). We were able to use paired end reads and copy number variations in the Illumina data to confirm the multiple breakpoints and copy number variations of the *mab-3* region (Figure 4B).

The biolistic-mediated insertion was located on contig tig00000045, which aligned to the right arm of chromosome III consistent with the published location for *ruIs32* (Wormbase). From the MinION read assembly, it appears that the insertion contains three copies of the *Ppie-1::GFP::H2B::pie*-1 transgene and two copies of the ampicillin gene from the plasmid and two

bioRxiv preprint doi: https://doi.org/10.1101/099143; this version posted January 8, 2017. The copyright holder for this preprint (which was not certified by peer review) is the author/funder, who has granted bioRxiv a license to display the preprint in perpetuity. It is made available under aCC-BY-NC-ND 4.0 International license.

partial copies of the *unc-119(+)* gene from the *unc-119* transgene. The structure of the insertion is complex, with the *unc-119(+)* sequence interspersed within the plasmid sequence suggesting a complex integration event (Figure 5A). Copy number changes and breakpoints in *pie-1* and *unc-119* were confirmed by the Illumina sequencing reads (Figure 5B). The integration event also appears to have generated a large duplication of approximately 2 Mb of DNA (chrIII:10,062,096-11,973,739) from the region near the insertion site (Figure 2). Given the position of the insertion, the wild type *unc-119* transgene should be genetically linked to the *unc-119(ed3)* mutation and should not be lost through outcrossing. Indeed, we were able to ascertain both the mutant and two wild type transgenic alleles of *unc-119* from the MinION contigs (Figure 5C).

Discussion

Advances in long read sequencing have opened new avenues for genome analysis. The relatively short sequencing reads produced by NGS allow for resequencing less complex, non-repetitive regions in well-characterized genomes. However, long sequence reads span repetitive regions and facilitate contiguous assemblies of large contigs. Similarly, long reads are essential for resolving complex chromosomal alterations such as those observed in tumour genomes. The major challenges previously limiting the use of long read TGS technology have been throughput, accuracy, and cost. The MinION sequencer has low equipment and consumable costs, and here we show that the MinION has achieved throughput and error rates that make it a viable option for the sequencing of novel genomes and genomes containing complex chromosomal rearrangements such as those observed in tumours. Continued advancements in both nanopore chemistry and basecalling will further improve throughput and accuracy. Additionally, with the advent of the high throughput ONT PromethION instrument genomes of larger sizes should be within easy reach.

We demonstrate here that the sequencing and *de novo* assembly of a large, low percent-GC (35.44), complex metazoan genome can be accomplished using MinION technology. We were able to assemble a near complete *C. elegans* genome with large contigs from less than 60-fold

bioRxiv preprint doi: https://doi.org/10.1101/099143; this version posted January 8, 2017. The copyright holder for this preprint (which was not certified by peer review) is the author/funder, who has granted bioRxiv a license to display the preprint in perpetuity. It is made available under aCC-BY-NC-ND 4.0 International license.

sequence coverage. MinION sequence read quality has increased to a level that 1D reads now achieve error rates <10% and result in more unique reads per flow cell.

Despite having higher error rates than NGS data, nanopore reads could be assembled into contigs with high concordance to the reference sequence. While consensus sequencing corrects for random sequencing errors, not all sequencing errors generated by MinION are random. Presently, MinION reads do not discern homopolymeric nucleotide tracts longer than 5 nucleotides. Consistent with this deficiency, the MinION assembled contigs did not contain any of the 396 >18 mer G-tracts known to be present in the *C. elegans* genome (Zhao et al. 2007). Pilon can improve the identity of homopolymeric tracts but not completely. Although homopolymeric runs were truncated in the MinION reads, the quality of sequence in their flanking regions was not affected. Illumina sequencing was more effective in sequencing homopolymeric tracts although we observed that Illumina reads were also affected by large G-tracts with lower read coverage in regions spanning G-tracts. Improvements in the ability to detect homopolymeric sequences from nanopore data are anticipated near-term.

For the purposes of this analysis, we assembled the genome using Canu alone and did not use manual finishing methods to bridge contigs. Assembled contigs were very large with an N50 contig size >1 Mb. A more contiguous genome assembly could be generated from the same data by using manual finishing approaches to bridge contigs. For example, it is clear from the LASTZ alignment that many of the contigs contain sequence overlaps between adjacent contigs. The genome assembly could be made more complete using long reads that extend from the ends of the contigs to find potential links between existing contigs resulting in a more contiguous genome assembly. The genome assembly could also be improved by changing the quality of the DNA sample before sequencing. Contig breakpoints were often in regions containing repetitive regions that were larger than the average read length. Increasing the number of reads longer than these repeat regions will facilitate the spanning of these regions. This could be accomplished by sequencing deeper or by preparing the genomic DNA to favour the formation of larger fragments.

bioRxiv preprint doi: https://doi.org/10.1101/099143; this version posted January 8, 2017. The copyright holder for this preprint (which was not certified by peer review) is the author/funder, who has granted bioRxiv a license to display the preprint in perpetuity. It is made available under aCC-BY-NC-ND 4.0 International license.

Chromosome rearrangements are common in tumours and the identification of rearrangements is important for tumour characterization and treatment. Detecting chromosome rearrangements such as duplications, deletions and translocations pose challenges for sequencing-based approaches. NGS can detect copy number changes and identify potential breakpoints. However, complex rearrangements with multiple breakpoints and duplications can prove difficult to reassemble from NGS reads. We demonstrate that long MinION reads provide context for assembly of duplicated rearranged sequence and can delineate complex chromosome rearrangements. MinION long reads offer the opportunity to cheaply identify genome rearrangements in tumours including the highly complex chromothripsis events which result in thousands of clustered localized chromosomal rearrangements (Leibowitz et al. 2015).

Our sequencing and assembly of the *C. elegans* genome demonstrates the advancing capabilities of the MinION sequencer. Throughput and accuracy of the MinION platform continues to improve and is approaching 5-10 Gb of sequence per flowcell, which would generate sufficient sequence to assemble the 100 Mb *C. elegans* genome. The long read capabilities of MinION nanopore sequencing facilitate unambiguous assembly of chromosome structure, thereby eliminating the need for physical mapping. These properties allow for sequencing of new genomes or tumour genomes with structural chromosome changes. Combining MinION and Illumina sequencing currently can delineate the structure of novel genomes with higher base-level certainty. Alternative techniques, for example, using nanopore only event based correction methods (Loman et al. 2015), offer improved accuracies independent of hybrid NGS sequence correction. Combining this with future improvements in basecaller performance is anticipated to further remove the need for SBS in regard to high sequence accuracy.

Acknowledgement

The authors would like to thank both Dr. Mark Akeson (MA) and Dr. Benedict Paten (BP) for supporting MJ and HEO, and for allowing use of the computer cluster to run assemblies and analyses. JRT and TPS thank the Canadian Institutes of Health Research (grant #10677) and Brain Canada Multi-Investigator Research Initiative Grant with matching support from Genome

bioRxiv preprint doi: https://doi.org/10.1101/099143; this version posted January 8, 2017. The copyright holder for this preprint (which was not certified by peer review) is the author/funder, who has granted bioRxiv a license to display the preprint in perpetuity. It is made available under aCC-BY-NC-ND 4.0 International license.

British Columbia, the Michael Smith Foundation for Health Research and the Koerner Foundation for funding. NJO and PH thank the Canadian Cancer Society (grant 702975). MJ and HEO thank the National Human Genome Research Institute of the US National Institutes of Health for funding their PI's under award numbers HG006321 (MA), HG007827 (MA), and U54HG007990 (BP). We also thank Oxford Nanopore Technologies for access to hardware, software and sequencing chemistries.

bioRxiv preprint doi: https://doi.org/10.1101/099143; this version posted January 8, 2017. The copyright holder for this preprint (which was not certified by peer review) is the author/funder, who has granted bioRxiv a license to display the preprint in perpetuity. It is made available under aCC-BY-NC-ND 4.0 International license.

References

Bessereau JL. 2006. Transposons in C. elegans. *WormBook*: 1-13.

C. elegans Sequencing Consortium. 1998. Genome sequence of the nematode C. elegans: a platform for investigating biology. *Science* **282**: 2012-2018.

Coulson A, Huynh C, Kozono Y, Shownkeen R. 1995. The physical map of the Caenorhabditis elegans genome. *Methods Cell Biol* **4896100433**: 533-550.

Coulson A, Kozono Y, Lutterbach B, Shownkeen R, Sulston J, Waterston R. 1991. YACs and the C. elegans genome. *Bioessays* **13**: 413-417.

Coulson A, Waterston R, Kiff J, Sulston J, Kohara Y. 1988. Genome linking with yeast artificial chromosomes. *Nature* **335**: 184-186.

Deamer D, Akeson M, Branton D. 2016. Three decades of nanopore sequencing. *Nature Biotechnology* 34:518-524.

Goodwin S, Gurtowski J, Ethe-Sayers S, Deshpande P, Schatz MC, McCombie WR. 2015. Oxford Nanopore sequencing, hybrid error correction, and de novo assembly of a eukaryotic genome. *Genome Res* **25(11)**:1750-1756.

Hodgkin J, Horvitz HR, Brenner S. 1979. Nondisjunction Mutants of the Nematode CAENORHABDITIS ELEGANS. *Genetics* **91**: 67-94.

Jain M, Fiddes IT, Miga KH, Olsen HE, Paten B, Akeson M. 2015. Improved data analysis for the MinION nanopore sequencer. *Nat Methods* **12**: 351-356.

Jain M, Olsen HE, Paten B, Akeson M. 2016. The Oxford Nanopore MinION: delivery of nanopore sequencing to the genomics community. Genome Biology **17**: 239-250.

Koren S, Walenz BP, Berlin K, Miller JR, Phillippy AM. 2016. Canu: scalable and accurate long-read assembly via adaptive k-mer weighting and repeat separation. *bioRxiv*.

Leibowitz ML, Zhang CZ, Pellman D. 2015. Chromothripsis: A New Mechanism for Rapid Karyotype Evolution. Annu Rev Genet. 49:183-211.

bioRxiv preprint doi: https://doi.org/10.1101/099143; this version posted January 8, 2017. The copyright holder for this preprint (which was not certified by peer review) is the author/funder, who has granted bioRxiv a license to display the preprint in perpetuity. It is made available under aCC-BY-NC-ND 4.0 International license.

Loman NJ, Quick J, Simpson JT. 2015. A complete bacterial genome assembled de novo using only nanopore sequencing data. *Nat Methods* **12(8)**:733-735.

Li H. 2013. Aligning sequence reads, clone sequences and assembly contigs with BWA-MEM. *arXiv [q-bio GN]*.

Meier B, Cooke SL, Weiss J, Bailly AP, Alexandrov LB, Marshall J, Raine K, Maddison M, Anderson E, Stratton MR, Gartner A, Campbell PJ. 2014. C. elegans whole-genome sequencing reveals mutational signatures related to carcinogens and DNA repair deficiency. *Genome Res.* **24**:1624–1636.

Norris AL, Workman RE, Fan Y, Eshleman JR, Timp W. 2016. Nanopore sequencing detects structural variants in cancer. *Cancer Biol Ther* **17(3)**:246–253.

Nurk S, Bankevich A, Antipov D, Gurevich A, Korobeynikov A, Lapidus A, Prjibelsky A, Pyshkin A, Sirotkin A, Sirotkin Y, et al. 2013. Assembling Genomes and Mini-metagenomes from Highly Chimeric Reads. In *Research in Computational Molecular Biology: 17th Annual International Conference, RECOMB 2013, Beijing, China, April 7-10, 2013. Proceedings*. (ed. Deng M, et al.), pp. 158-170. Springer Berlin Heidelberg, Berlin, Heidelberg.

Thompson O, Edgley M, Strasbourger P, Flibotte S, Ewing B, Adair R, Au V, Chaudhry I, Fernando L, Hutter H, et al. 2013. The million mutation project: A new approach to genetics in Caenorhabditis elegans. *Genome Res*. **23(10)**:1749-62.

Wei S, Williams Z. 2016. Rapid short-read sequencing and aneuploidy detection using MinION nanopore technology. *Genetics* **202**:37–44.

Walker BJ, Abeel T, Shea T, Priest M, Abouelliel A, Sakthikumar S, Cuomo CA, Zeng Q, Wortman J, Young SK, et al. 2014. Pilon: an integrated tool for comprehensive microbial variant detection and genome assembly improvement. *PLoS One* **9**: e112963.

Youds JL, O'Neil NJ, Rose AM. 2006. Homologous recombination is required for genome stability in the absence of DOG-1 in *Caenorhabditis elegans. Genetics* 2006 Jun;173(2):697-708.

Zhao Y, O'Neil NJ, Rose AM. 2007. Poly-G/poly-C tracts in the genomes of Caenorhabditis. *BMC Genomics* **8**: 403.

bioRxiv preprint doi: https://doi.org/10.1101/099143; this version posted January 8, 2017. The copyright holder for this preprint (which was not certified by peer review) is the author/funder, who has granted bioRxiv a license to display the preprint in perpetuity. It is made available under aCC-BY-NC-ND 4.0 International license.

Figure Legends

Figure 1: Dot plots of LASTZ alignments on MinION Pilon polished contigs to the *C. elegans* reference chromosomes. * denotes contig that aligns to chromosome II and V.

Figure 2: MinION read coverage (log scale) aligned to reference genome. Note the duplication between 10,062,096 and 11,973,739 on chromosome III.

Figure 3: LASTZ alignments of MinION contigs to C. elegans reference chromosomes. Discontinuities are due to contigs mapping to two different chromosomes. We have included these hybrid contigs on both chromosomes to allow for alignment. These hybrid contigs are most likely the result of contig assembly errors in highly repetitive regions.

Figure 4: Elucidating the structure of the complex *him-9(e1487)* acetaldehyde-induced mutation. (A) Schematic of the 40 kb insertion of the *mab-3* region into the *xpf-1* gene based on contig 1701. The insertion structure suggests a mutation event in which the insertion was duplicated to generate an inverted repeat of the *mab-3* region and the insertion point with *xpf-1* (in red). (B) The *mab-3* region with breakpoints denoted with arrows. Breakpoints detected by MinION are corroborated by Illumina read coverage and paired-end read alignment.

Figure 5: Elucidating the *ruIs32* insertion. (A) Dot plot of the contig 45 region that aligns with the pJH4.52 plasmid (pJH4.52 was used because pAZ132 sequence is not available. pAZ132 was derived from pJH4.52) and the *unc-119* gene. (B) Illumina read data illustrating the breakpoints and copy number changes identified in the MinION data. (C) The sequence of *unc-119* identified in the MinION data.

bioRxiv preprint doi: https://doi.org/10.1101/099143; this version posted January 8, 2017. The copyright holder for this preprint (which was not certified by peer review) is the author/funder, who has granted bioRxiv a license to display the preprint in perpetuity. It is made available under aCC-BY-NC-ND 4.0 International license.

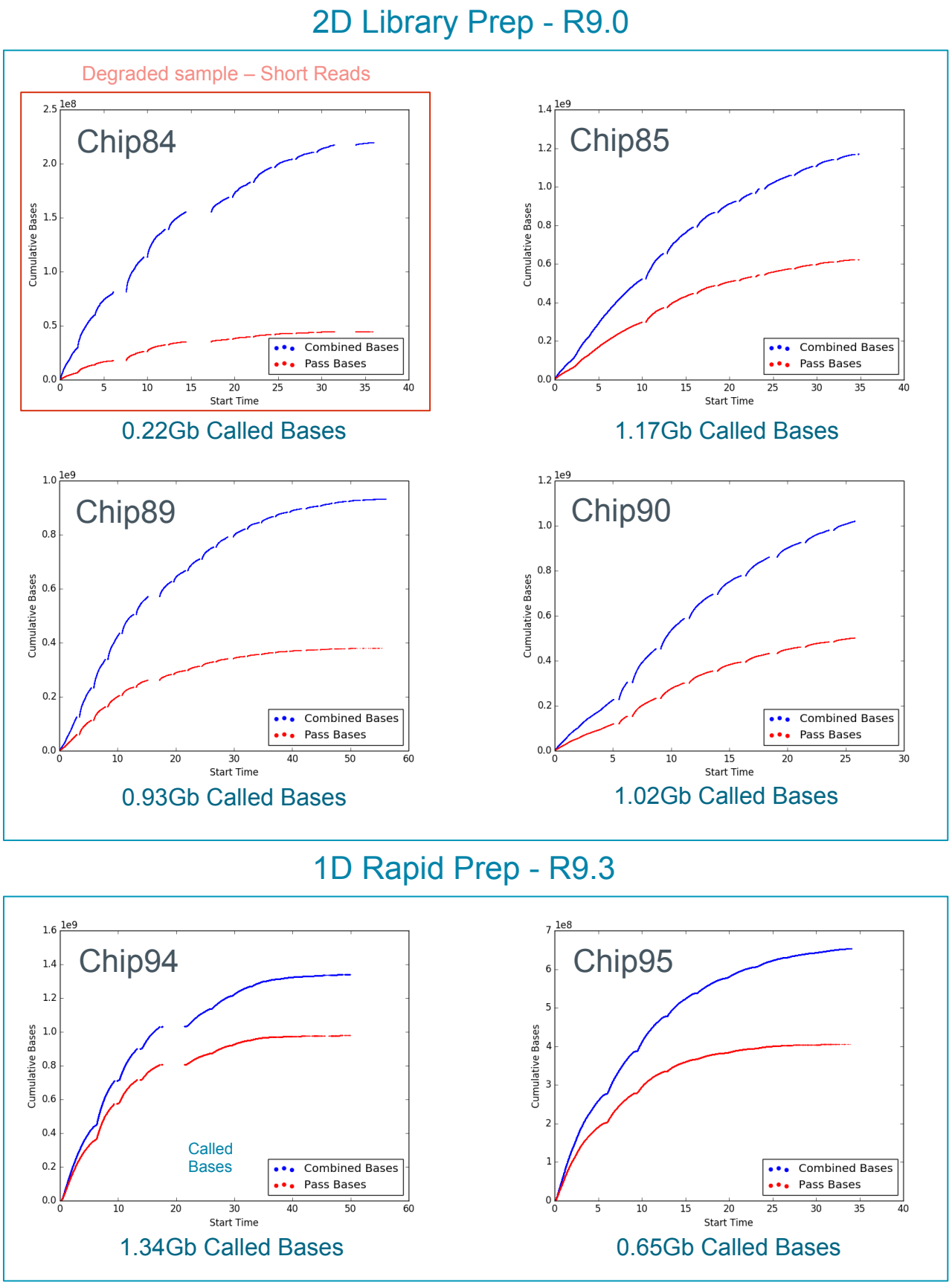

Figure 1. MinION Sequencing Run Summaries. Called base yield accumulations from MinION flowcell sequencing runs.

	Chip84	Chip85	Chip89	Chip90	Chip94	Chip95
Library Kit	SQK-NSK007	SQK-NSK007	SQK-NSK007	SQK-NSK007	SQK-RAD001	SQK-RAD001
Flowcell ID	FAD11292	FAD11271	FAD11308	FAB23558	FAD24831	FAD24186
Pore Type	R9.0	R9.0	R9.0	R9.0	R9.3	R9.3
Genomic DNA Start Material	749ng	1650ng	1978ng	1978ng	864ng into 20ul	1152ng into 20ul
Volume Loaded	12ul 0hrs, 12ul 0.5hrs	12ul 0hrs,	12ul 0hrs	6ul 0hrs, 6ul 24hrs	11ul 0hrs, 11ul 24hrs	11ul 0hrs, 11ul 24hrs
Preseq Mix Conc.	7.14ng/ul	5.34ng/ul	8.56ng/ul	8.56ng/ul	na	na
PlatQC Pores	1155//486,397,217,55	1036//467,357,170,42	1060//428,340,222,70	1404//489,444,330,141	1277//494,423,271,89	1361//504,448,312,97
Total Reads	**198,913**	**184,600**	**142,374**	**155,508**	**268,004**	**161,378**
Pass Reads	36,949	68,204	34,816	54,892	180,938	89,376
Av Template Read Length	831	4,052	4,486	4,430	5,001	4,049
Av Complement Read Length	272	2,281	2,059	2,125	na	na
Av 2D Read Length	171	2,207	1,826	1,972	na	na
Max Pass Template Read size	9,460	29,221	44,484	32,910	108,915	123,159
Max Pass Complement Read size	9,130	28,814	34,881	31,458	na	na
Max Pass 2D Read size	9,740	29,681	44,405	33,553	na	na
Top 25% Templates >	904	6,106	6,858	6,622	6,390	4,717
Top 25% Complements >	305	4,233	2,721	2,896	na	na
Top 25% 2D >	273	4,454	1,987	2,533	na	na
Total Called bases	**219,411,804**	**1,169,061,304**	**931,927,653**	**1,019,278,312**	**1,340,369,063**	**653,447,905**
2D Pass Bases	22,208,070	323,598,976	195,759,566	258,533,514	na	na
2D fail Bases	11,877,828	83,731,694	64,225,734	48,089,637	na	na
2D Bases	34,085,898	407,330,670	259,985,300	306,623,151	na	na
Base Calling	2D Chimera 1.22.10	2D Chimera 1.22.10	2D Chimera 1.22.10	2D Chimera 1.22.10	1D Chimera 1.22.10	1D Chimera 1.22.10
MinKNOW version	0.51.3.55	0.51.3.55	0.51.3.55	0.51.3.55	1.0.5	1.0.5
Comment	Small Frags degraded Library			SpotON Flowcell		

Table 1. MinION Sequencing Data Summary. Individual library preparation and run statistics for MinION sequencing of *C.elegans him-9* mutant.

bioRxiv preprint doi: https://doi.org/10.1101/099143; this version posted January 8, 2017. The copyright holder for this preprint (which was not certified by peer review) is the author/funder, who has granted bioRxiv a license to display the preprint in perpetuity. It is made available under aCC-BY-NC-ND 4.0 International license.

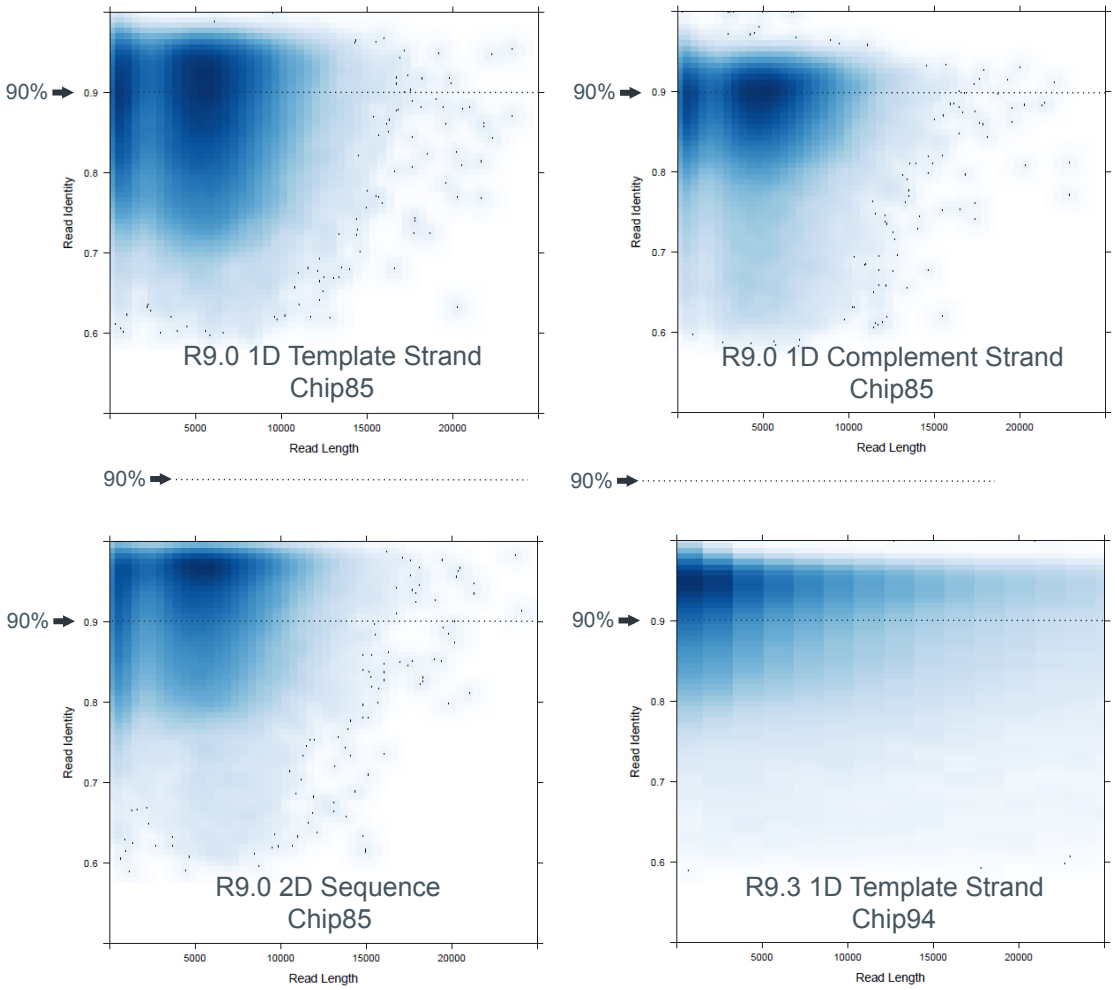

Figure S1. MinION Individual Read Accuracies vs Read Length. Example plots for both R9.0 2D and R9.3 1D chemistries. Individual pass read accuracies from aligned regions calculated using bwa alignment to the reference sequence and plotted against individual read length.

bioRxiv preprint doi: https://doi.org/10.1101/099143; this version posted January 8, 2017. The copyright holder for this preprint (which was not certified by peer review) is the author/funder, who has granted bioRxiv a license to display the preprint in perpetuity. It is made available under aCC-BY-NC-ND 4.0 International license.

	Reads	Percentage
Total PF	28,156,060	100.00
Paired	28,082,998	99.74
Read 1	14,041,499	49.87
Read 2	14,041,499	49.87
Aligned	26,581,603	94.41
Properly Paired	26,343,266	99.10
Singletons	69,881	0.26
Secondary Alignments	73,062	0.27
Supplementary Alignments	0	0.00
Duplicates	584,096	2.20

Table 2: Illumina sequencing Read Data

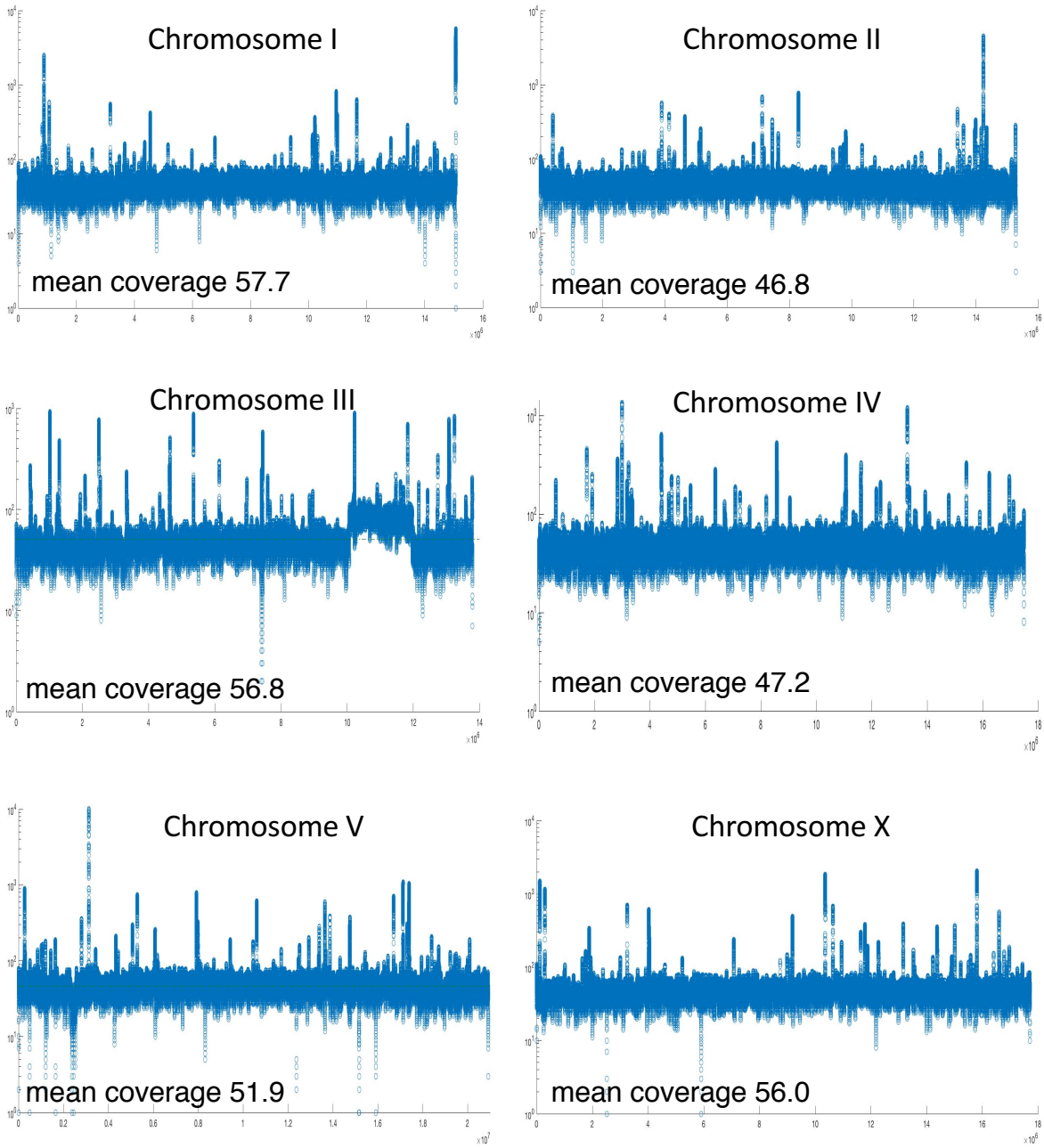

Figure 2: MinION read coverage (log scale) aligned to reference genome. Note the duplication between 10,062,096 and 11,973,739 on chromosome III.

bioRxiv preprint doi: https://doi.org/10.1101/099143; this version posted January 8, 2017. The copyright holder for this preprint (which was not certified by peer review) is the author/funder, who has granted bioRxiv a license to display the preprint in perpetuity. It is made available under aCC-BY-NC-ND 4.0 International license.

	Canu(HQ)	Canu(All)	Canu(HQ)+Pilon	Canu(All)+Pilon	Illumina (>Q30)
Total Bases	2,184,632,490	6,341,521,060	2,184,632,490	6,341,521,060	4,022,919,599
Nanopore data >1kb	2,117,363,533	6,025,477,392	2,117,363,533	6,025,477,392	
Illumina data			8,036,947,435	8,036,947,435	3,545,850,569
Unassembled Data	433,367,624	1,086,588,269			49,124,114
# contigs	308	294	308	294	38,645
Total Assembly (bp)	101,997,097	103,164,837	104,756,867	106,194,296	117 Mb
N50 (Mb)	1.30	1.17	1.33	1.21	0.026
Average Contig Size (Kb)	331	351	340	361	3
Average Read Length	6,160	5,528			~127 (141 p1, 112 p2)
Read N50	8,692	7,672			~169 (181 p1, 157 p2)
Largest Contig (Mb)	5,018,199	4,573,586	5,130,018	4,688,558	1,801,795
Genome Fraction (%)	92.37	92.84	98.13	98.92	94.03
Total Aligned Length	91,240,752	91,290,952	99,568,344	100,288,126	94,504,201
#Mismatches	34,610	23,631	51,131	50,146	29,289
#Indels	1,551,278	1,761,037	64,364	61,304	6,831
Indels length	2,413,421	2,699,872	185,846	181,052	34,903
GC%	36.36	36.44	36.00	36.07	37.43
Identity to reference	97.31%	97.01%	99.76%	99.77%	99.93%

HQ	2D pass from Chip84,85,89,90 and 1D pass from Chip94,95
All	All reads (1D template, 1D complement & 2D from pass and fail)

Table 3. *C.elegans him-9* mutant Genome Assemblies and Polishing. Different genome assemblies using Nanopore, Illumina and combined data sets. (HQ) 2D pass from Chip84, 85, 89, 90 and 1D pass from Chip94, 85. (All) All reads, 1D template, 1D complement & 2D from pass and fail catagories.

Chromosome I			Chromosome II			Chromosome III			Chromosome IV			Chromosome V			Chromosome X			Mitochondrial chromosome		
CONTIG	LENGTH	PILON LENGTH	CONTIG	LENGTH	PILON LENGTH	CONTIG	LENGTH	PILON LENGTH	CONTIG	LENGTH	PILON LENGTH	CONTIG	LENGTH	PILON LENGTH	CONTIG	LENGTH	PILON LENGTH	CONTIG	LENGTH	PILON LENGTH
0128	641,577	667,188	0093	1,404,993	1,452,753	1829	322,164	335,057	0069	57,949	59,969	1815	289,924	300,768	0291	105,703	110,238	111	26,495	26,994
0162	249,830	261,633	0066	1,825,969	1,884,875	1827	145,979	151,731	0064	1,470,161	1,523,240	1816	47,237	47,480	1808	968,329	995,374			
0146	101,839	105,941	0190	145,554	149,288	0157	449,989	464,710	1775	23,228	23,545	1817	827,816	855,414	1839	3,895	3,979			
0155	90,893	94,925	0113	522,805	538,113	0044	286,814	299,041	1774	152,421	158,647	1793	1,083,739	1,121,912	1791	1,525,866	1,573,864			
0060	910,770	955,944	1732	1,147,314	1,180,765	1753	106,886	110,089	0022	309,830	325,753	0039	1,999,640	2,060,681	0056	118,963	126,367			
0144	285,340	305741	1776	1,333,788	1,365,313	0063	1,054,603	1,105,484	0084	936,097	976,525	1802	937,727	968,247	0089	48,192	49,234			
0041	147,174	159,766	1777	15,658	15,848	0121	780,480	817,746	0019	475,203	505,301	1803	34,408	34,549	1759	836,347	862,726			
1812	597,398	614,699	1778	2,891,883	2,957,296	0031	1,971,186	2,029,091	1787	1,055,217	1,091,923	1742	793,648	813,478	1757	174,755	180,694			
1811	19,219	19,306	1789	15,231	15,270	1735	55,591	55,699	0029	1,325,883	1,363,306	1765	18,063	18,253	1730	1,014,182	1,041,746			
1725	4,573,586	4,688,558	0023	595,982	609,952	1736	2,020,242	2,069,914	1750	889,415	913,229	1807	27,100	27,102	0456	11,254	11,286			
1729	318,637	327,171	1766	2,478,930	2,559,627	1798	159,446	162,596	1751	39,749	40,436	1835	22,957	23,062	0075	1,766,377	1,813,766			
1727	83,750	85,600	0009	1,108,459	1,153,611	1783	2,577,988	2,640,414	0042	627,979	642,707	1764	873,000	893,363	0211	205,924	211,400			
0018	750,497	770,051	0119	327,432	341,061	0040	447,466	460,463	1796	1,195,712	1,223,010	1762	967,542	989,686	0102	1,178,956	1,207,894			
0136	681,659	708,475	1819	18,180	18,661	0065	1,618,827	1,687,451	1795	18,456	18,575	1810	80,862	82,488	1780	848,498	870,998			
0152	422,339	438,644	1806	371,509	383,023	1790	771,310	804,548	1794	460,691	471,631	1761	19,250	19,316	1779	23,740	24,063			
0097	1,353,294	1,397,343	1805	24,717	25,461	1836	17,002	17,100	0099	1,275,584	1,304,238	0092	505,374	516,537	1744	259,389	265,556			
0156	394,056	410,474	1804	550,140	573,165	1788	692,834	717,085	0124	649,249	663,972	1821	328,510	335,880	0114	898,142	919,234			
0068	110,325	116,857				1758	3,917	3,923	1740	102,549	104,785	1737	1,751,778	1,788,507	0074	1,406,913	1,439,548			
1813	1,030,425	1,069,619				0808	7,998	8,057	0011	944,601	967,191	1739	1,874,708	1,915,981	1734	111,328	114,321			
1814	75,058	75,451							0003	2,682,200	2,772,593	0107	1,110,630	1,136,009	1767	2,448,979	2,515,054			
									1771	1,395,592	1,441,393	0095	1,073,058	1,099,497	1769	526,550	540,649			
									0055	972,204	999,639	1801	1,916,623	1,966,771	1745	23,913	24,056			
									1770	24,088	24,306	0015	381,581	391,181	1746	2,477,698	2,555,070			
									1773	298,435	308,756	1826	249,592	254,471	1747	6,362	6,364			
									0161	105,733	109,044	1824	136,416	138,132	1748	244,817	252,069			
									1760	694,777	726,700	1763	19,006	19,356						
									0081	710,949	738,400	1785	813,298	843,246						
									0123	877,321	907,738	1756	173,877	179,974						
												0017	171,054	177,803						
												0147	64,693	67,991						
												1823	350,901	365,730						
												0165	208,425	218,028						
												0175	167,421	172,916						
												0142	571,657	596,057						
												0117	922,679	955,919						
Total CONTIG	12837666	13273386		14,778,544	15,224,082		13,490,722	13,940,199		19,771,273	20,406,552		20,814,194	21,395,785		17,235,07	17,715,550		26,495	26,994
Reference bp		15,072,434			15,279,421			13,783,801			17,493,829			20,924,180			17,718,942			13,794

Table 4. Worm Contigs

bioRxiv preprint doi: https://doi.org/10.1101/099143; this version posted January 8, 2017. The copyright holder for this preprint (which was not certified by peer review) is the author/funder, who has granted bioRxiv a license to display the preprint in perpetuity. It is made available under a CC-BY-NC-ND 4.0 International license.

bioRxiv preprint doi: https://doi.org/10.1101/099143; this version posted January 8, 2017. The copyright holder for this preprint (which was not certified by peer review) is the author/funder, who has granted bioRxiv a license to display the preprint in perpetuity. It is made available under aCC-BY-NC-ND 4.0 International license.

	Contigs after Pilon		
Chromosome (Size in bp)	Pairwise Identity (%)	Identical Sites (%)	Reference Coverage (%)
I (15,072,434)	80.9	95.0	99.8
II (15,279,421)	83.3	96.1	99.9
III (13,783,801)	84.5	94.4	99.2
IV (17,493,829)	85.3	96.3	99.8
V (20,924,180)	85.7	96.0	99.2
X (17,718,942)	84.1	97.5	99.5
Mito (13,794)	98.5	98.8	100

Table 5. LASTZ alignment of contigs to the Six chromosomes and the *C.elegans* mitochondrial genome.

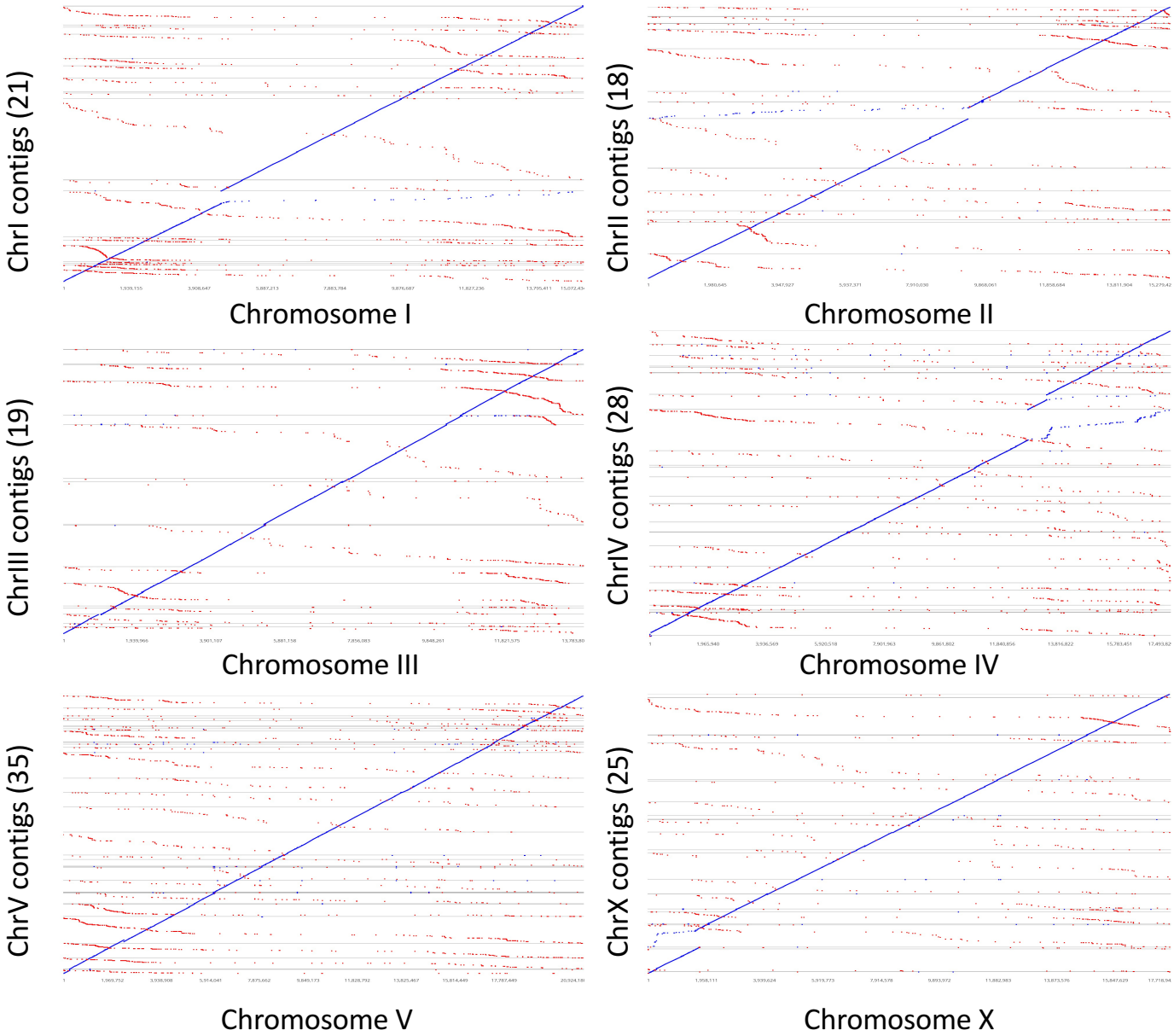

Figure 3: LASTZ alignments of MinION contigs to *C. elegans* reference chromosomes.

bioRxiv preprint doi: https://doi.org/10.1101/099143; this version posted January 8, 2017. The copyright holder for this preprint (which was not certified by peer review) is the author/funder, who has granted bioRxiv a license to display the preprint in perpetuity. It is made available under aCC-BY-NC-ND 4.0 International license.

MinION Contigs					Reference Genome			
Contig Name	Chr	Length	% Pairwise Identity	% Query Coverage	Chr	Length	% Pairwise Identity	% Query Coverage
tig00000076	I	1,610	99.6	100	I	1,611	99.6	100
tig00000097	I	852	99.3	53	I	852	99.3	53
tig00000097	I	741	99.7	46	I	741	99.7	46
tig00000148	I	1,532	98.5	100	I	1,611	99.6	100
tig00000066	II	1,598	98.8	100	II	1,612	99.8	100
tig00000093	II	1,598	98.9	100	II	1,611	99.9	100
tig00000093	II	1,608	99.7	100	II	1,612	99.6	100
tig00001732	II	862	99.7	53	II	861	99.7	53
tig00001766	II	1,600	98.8	100	II	1,611	99.6	100
tig00001766	II	1,605	99.2	100	II	1,611	99.6	100
tig00001778	II	1,605	99.3	100	II	1,611	99.8	100
tig00001778	II	1,609	99.1	100	II	1,611	99.4	100
tig00000009	II	1,473	99.1	91	II	1,472	99.3	91
tig00000063	III	1,613	99.4	100	III	1,611	99.6	100
tig00001790	III	1,599	99.1	100	III	1,611	99.7	100
tig00000055	IV	1,610	99.6	100	IV	1,610	99.6	100
tig00000084	IV	1,582	98.0	100	IV	1,611	99.6	100
tig00000099	IV	1,608	99.4	100	IV	1,611	99.6	100
tig00001760	IV	1,602	99.2	100	IV	1,611	99.7	100
tig00001793	V	1,511	99.0	94	V	1,522	99.7	94
tig00001793	V	1,603	99.2	100	V	1,611	99.7	100
tig00001785	V	1,595	98.6	100	V	1,611	99.4	100
tig00000017	V	1,609	99.6	100	V	1,612	99.3	100
tig00001801	V	1,607	99.3	100	V	1,611	99.6	100
tig00001737	V	725	98.9	45	V	729	99.5	45
tig00001737	V	1,610	99.1	100	V	1,610	99.6	100
tig00000005	V	1,504	99.3	94	V	1,508	99.6	94
tig00000039	V	1,602	99.1	100	V	1,611	99.8	100
tig00000039	V	1,595	98.8	100	V	1,611	99.8	100
tig00000039	V	1,602	99.3	100	V	1,611	99.6	100
tig00001739	V	1,596	98.8	100	V	1,611	99.6	100
tig00000211	X	1,602	99.1	100	X	1,611	99.6	100
tig00000074	X	1,613	99.3	100	X	1,611	99.4	100

Table 6. Tc1 transposon numbers, locations and match compared to reference Genome.

bioRxiv preprint doi: https://doi.org/10.1101/099143; this version posted January 8, 2017. The copyright holder for this preprint (which was not certified by peer review) is the author/funder, who has granted bioRxiv a license to display the preprint in perpetuity. It is made available under aCC-BY-NC-ND 4.0 International license.

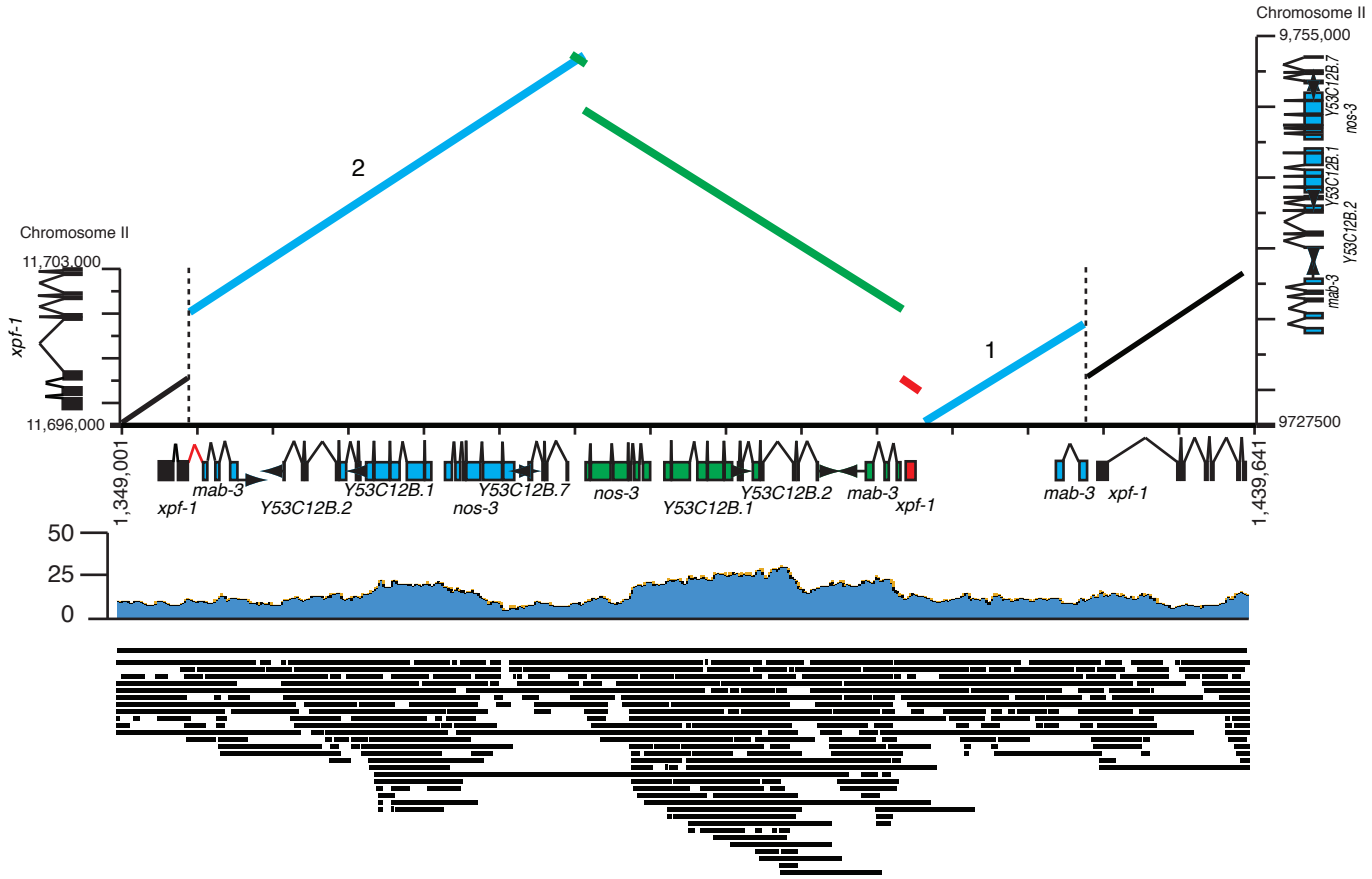

Figure 4A: Schematic of the 40kb complex insertion of *mab-3* region into the *xpf-1* gene. The insertion is in contig 1766. The insertion is an inverted repeat.Shown below are selected MinION reads mapping to the region spanning the various breakpoints.

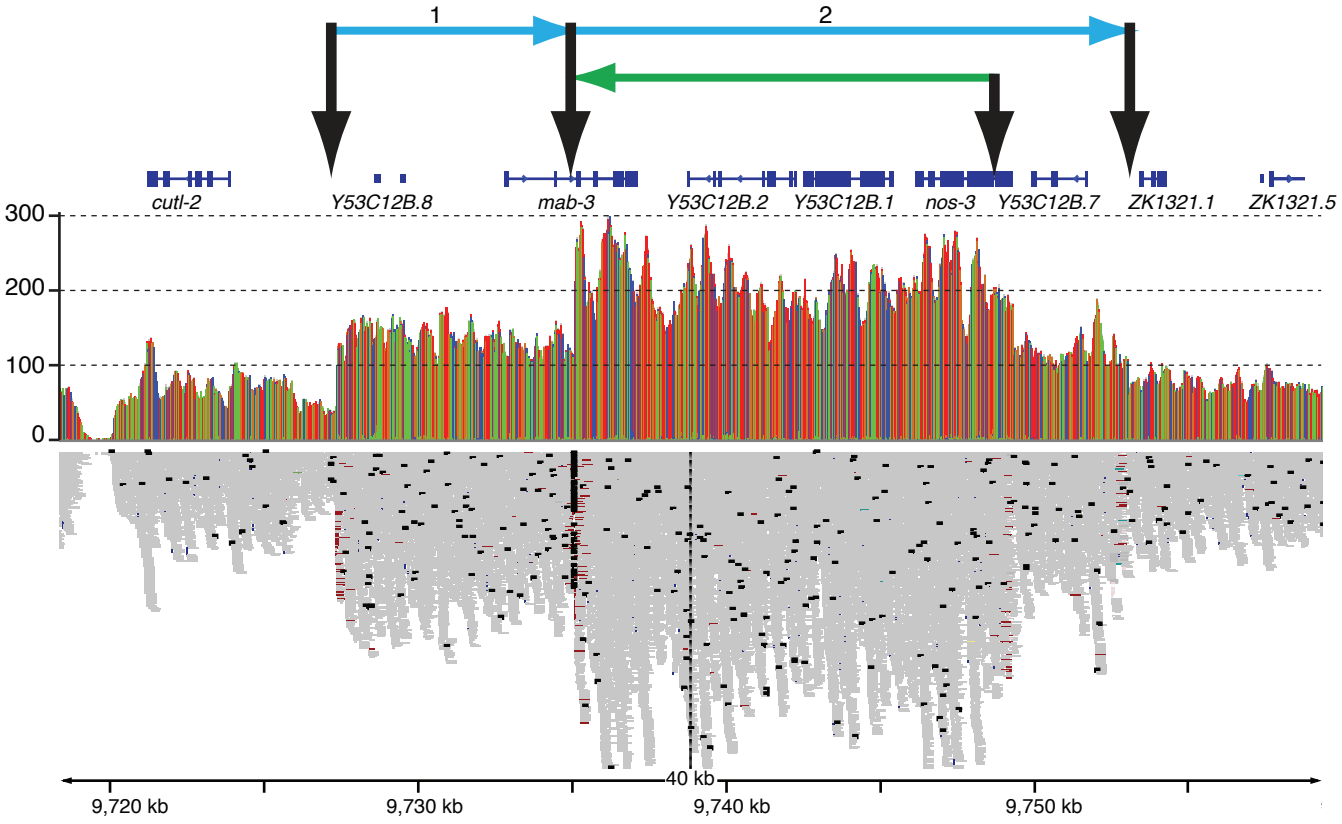

Figure 4B: The mab-3 region showing breakpoints detecting in MinION sequencing data and Illumina read coverage.

bioRxiv preprint doi: https://doi.org/10.1101/099143; this version posted January 8, 2017. The copyright holder for this preprint (which was not certified by peer review) is the author/funder, who has granted bioRxiv a license to display the preprint in perpetuity. It is made available under aCC-BY-NC-ND 4.0 International license.

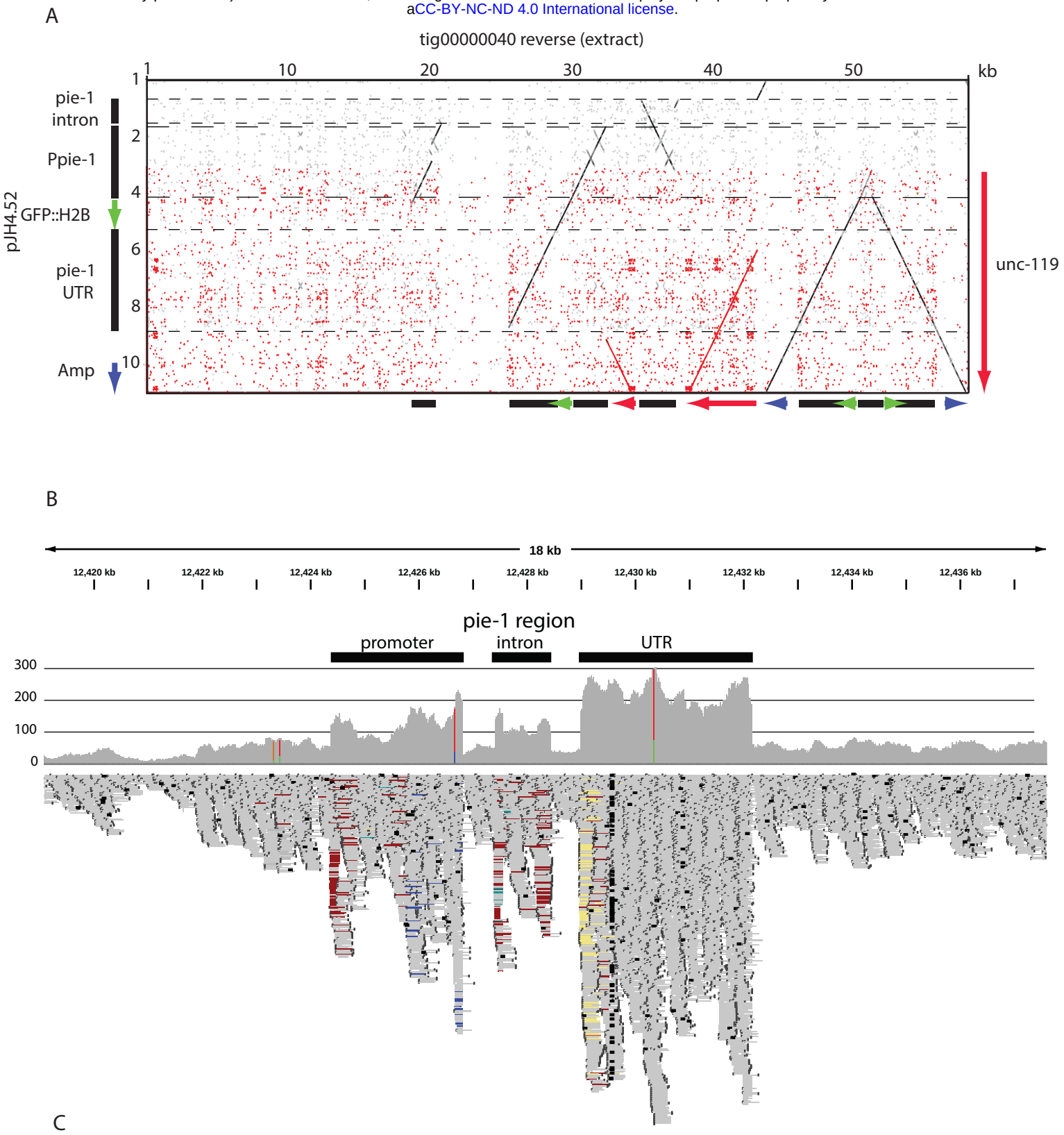

Figure 5. Elucidating the *ruIs32* insertion. (A) Dot plot of the contig 45 region that aligns with the pJH4.52 plasmid (pJH4.52 was used because pAZ132 sequence is not available. pAZ132 was derived from pJH4.52) and the *unc-119* gene. (B) Illumina read data illustrating the breakpoints and copy number changes identified in the MinION data. (C) The sequence of *unc-119* identified in the MinION data.